Shadow wave function for liquid and solid ^{3}He

F. Pederiva
Laboratorio di Fisica Computazionale, Dipartimento di Fisica, Universitá di Trento, I-38050 Povo, Trento, Italy

S. A. Vitiello
International Centre for Theoretical Physics, I-34014 Trieste, Italy
and Scuola Internazionale Superiore di Studi Avanzati, International School for Advanced Studies, I-34014 Trieste, Italy

K. Gernoth
Universität zu Köln, Institut für Theoretische Physik, D-50937, Köln, Germany
and Scuola Internazionale Superiore di Studi Avanzati, International School for Advanced Studies, I-34014 Trieste, Italy

S. Fantoni
International Centre for Theoretical Physics, I-34014 Trieste, Italy
and Scuola Internazionale Superiore di Studi Avanzati, International School for Advanced Studies, I-34014 Trieste, Italy

L. Reatto
Dipartimento di Fisica and Instituto Nazionale di Fisica della Materià, Università di Milano, Milano, Italy
(Received 5 July 1995)

The ideas of the shadow wave function are applied to construct a variational wave function to describe the liquid and the solid phase of a system that obeys Fermi statistics. The shadow variables are introduced in the symmetric correlating factor. The antisymmetric part is a standard determinant of plane waves modified by backflow effect. Variational Monte Carlo calculations for ^{3}He provide ground-state energies in the liquid phase at the level of the most elaborate trial function available in the literature. With this wave function, properties like translational invariance and antisymmetry under particle interchange are maintained even in the crystalline phase. [S0163-1829(96)08321-X]

I. INTRODUCTION

The shadow wave function (SWF) (Refs. 1–3) has shown to be a powerful tool in the investigation of quantum solids and liquids obeying Bose statistics. In the context of variational Monte Carlo (VMC) calculations, it has allowed for studying many properties of superfluid and solid ^{4}He: the crystallization,[3,4,10] the excitation spectrum both at zero[5] and at finite temperature,[6,7] the properties of the roton at finite temperature,[8] and the liquid-solid coexistence.[9] In this work we apply the shadow wave function ideas to the ground state of a Fermi system. In this way we obtain a wave function that satisfies the properties of translational invariance and antisymmetry under particle exchange even in the solid phase.

In the shadow wave function particles are correlated by pair terms in the form of a Jastrow factor and indirectly, via a coupling to subsidiary variables, the shadows. The shadow variables are also correlated between themselves by a Jastrow factor. Integration over these shadow variables introduces implicitly correlations between the particles not only at the pair level but also via triplet, quadruplet, and higher order terms. At large enough density these many body correlations become strong enough that the particles become localized and a crystalline solid becomes stable. In this way one has a wave function which is translationally invariant, while the system displays a spontaneously broken translational symmetry.

The standard trial wave functions for the ground state ψ_0 of a Fermi fluid, like liquid ^{3}He, is usually written as the product of two factors.[11] The first is symmetric under interchange of particles, and often has a Jastrow form. Better results are obtained if this factor contains also explicit triplets terms.[12–14] The second factor is antisymmetric, and of the form of a Slater determinant of plane waves. In the absence of spin-flip terms both in the Hamiltonian and in the correlations, the Slater determinant can be decomposed in the product of two such determinants, one for particles with spin up and one for those of spin down. Even better results are obtained if the plane waves are modified by the so-called backflow terms.[12–14] These wave functions go under the name of Jastrow-Slater (JS), (Jastrow+triplet)-Slater [(J+T)S], and (Jastrow+triplet)-Slater-backflow [(J+T)SB], respectively. Shadow variables can be introduced in two main different ways.[15,16] In the first[16] it is the symmetric correlating factor which is augmented by a shadow factor, and the antisymmetric part remains written in terms of the particle variables. In this case the nodal structure remains exactly the same as that of a standard wave function, as for instance Slater or Slater backflow. The shadow variables introduce only many body correlations of symmetric character. The second possibility[15] is to write the determinant in terms of the shadow variables. In this case the nodal surface for the particle variables is no more that of the Slater determinant, and the implicit many body correlations introduced by the shadow variables are not limited to the symmetric ones.

In this paper we present the computation for ^{3}He based on the shadow wave function. We have adopted the first choice, the one with symmetric shadows. This is computationally much easier to study than the other choice, and it allows for addressing two main issues. From the study of ^{4}He it is known that at equilibrium density the triplet correlations have an important role, but higher order correlations do not. The situation is quite different when the density increases. At the freezing point the energy upperbound given by the shadow wave function is significantly lower than that obtained with wave functions containing fully optimized Jastrow and triplets terms.[17,18] This means that terms beyond the triplet ones must be of comparable importance. It is known that also in ^{3}He triplet terms are important at equilibrium density to obtain a quantitative understanding of the equation of state, and other fundamental properties of the liquid, such as the momentum distribution and the structure factor. With the present computation we want to see if shadow variables are able to represent the effects of such triplet terms and if there is any evidence of higher order correlations from the symmetric part becoming important at densities close to the freezing point, as in ^{4}He.

The more relevant question has to do with the possibility that the symmetric many body correlations introduced by the shadow variables are able to give a stable crystalline solid phase. Helium solids were first described as a product of single particle Gaussians by Nosanow and Shaw.[19] Much better results were obtained by Nosanow[20] when short-range correlations were introduced in this wave function through a correlation factor of the Jastrow form. VMC calculations for crystal ^{3}He where first performed by Hansen and Levesque[21] using a Nosanow-Jastrow wave function. Similar results have been obtained later on by Ceperley *et al.*,[22] who considered also a determinant of Gaussians in addition to a simple product of one-body Nosanow terms. All these calculations were based on wave functions that have factors breaking the translational invariance, and *a priori* equilibrium positions for the atoms have to be assumed. In fact, these factors, products of Gaussian one-body terms, constrain particles to remain around the assumed equilibrium positions forming a regular lattice. Although much useful information as obtained using such procedure, this class of wave functions have precluded the investigation of many interesting phenomena. The crystallization of a liquidlike configuration and the solid-liquid coexistence phase are typical examples that cannot be studied by imposing *a priori* equilibrium positions. On the other hand, a simple wave function of the Jastrow form together with an antisymmetrization factor, although being able to give rise to a crystal, would give a crystal with too tightly localized particles, providing an unacceptable description of the system.

Our computation shows that with symmetric shadows one can obtain a stable crystal without any one-body term that localize particles in a given *a priori* lattice, still leaving the correct antisymmetry of the wave function. We find also evidence for crystallization when the system is started from a liquidlike configuration. The most important outcome of our results is that the shadow wave function we propose to describe both liquid and solid ^{3}He, can therefore certainly be used to perform realistic studies of the liquid solid coexistence and interface.

The plan of the paper is the following. The trial wave function is described in Sec. II. Section III discusses the variational Monte Carlo method used in the calculation. The results are presented in Sec. IV. The last section is devoted to conclusions.

II. THE FERMI SHADOW TRIAL WAVE FUNCTION

Our trial wave function Ψ_F contains both the many-body correlations of the shadow type and the backflow correlations. It consists in the product of the bosonic SWF $\Psi_B(R)$, $R \equiv \{\mathbf{r}_i | i=1,\ldots,N\}$, by a factor $\Phi(R)$ embodying the antisymmetry property under particle interchange:

$$\Psi_F(R) = \Psi_B(R)\Phi(R). \tag{1}$$

Since we are modeling ^{3}He at $T=0$ K in the normal phase, we take $\Phi(R)$ as the antisymmetrized product of single particle orbitals, $\Phi(R) = \{\mathcal{A}\Pi\,\phi_{\boldsymbol{\kappa}}(i) | i=1,\ldots,N; k \leqslant k_F\}$, where $\mathcal{A}$ is the antisymmetrization operator $\boldsymbol{\kappa}$ denotes both the $\mathbf{k}$ vector and the spin state, and k_F the Fermi momentum. The single particle wave functions are taken as plane waves modified by backflow correlations

$$\phi_{\kappa}(i) = \exp\left[i\mathbf{k}\cdot\left(\mathbf{r}_i + \lambda_B \sum_{l\neq i} \eta(r_{il})\mathbf{r}_{il} \right)\right]\xi(i), \tag{2}$$

where $\eta(r)$ is the backflow function that correlates particle i with the remaining ones of the system, $\mathbf{r}_{il} = \mathbf{r}_i - \mathbf{r}_l$, and $\xi(i)$ represents the spin state of particle i. For an unpolarized system of N particles, there are $N/2$ of them with spin-up and an equal number with spin-down. Since $\Psi_B(R)$ does not contain spin-flip correlations, in the calculation of the expectation value of any spin-independent operator, $\Phi(R)$ of Eq. (1) can be written as

$$\Phi(R) = \left\{ \det_{\uparrow}[\phi_{\kappa}(i)]\det_{\downarrow}[\phi_{\kappa}(j)] \,\middle|\, i=1,\ldots,\frac{N}{2}; \right.$$
$$\left. j=\frac{N}{2}+1,\ldots,N; k \leqslant k_F \right\}, \tag{3}$$

namely the product of two Slater determinants, one for each spin state of the particles. We choose $\eta(r)$ to be of the form[12]

$$\eta(r) = \left(\frac{r-R_B}{R_B}\right)^3 \exp\left[-\left(\frac{r-r_B}{w_B}\right)^2 \right], \tag{4}$$

where λ_B, r_B, and w_B are variational parameters; R_B is taken as half of the simulation cell. The bosonic term of $\Psi_F(R)$ in Eq. (1) is of the shadow type, and is given by

$$\Psi_B(R) = \int dS K(R,S)\psi_s(S), \tag{5}$$

where $S \equiv \{\mathbf{s}_i | i=1,\ldots,N\}$ denote the shadow variables, that are correlated by $\psi_s(S)$. The kernel $K(R,S)$ consists of a product of a function $\psi(R)$, correlating the particles, and a function $\Theta(R,S)$ binding the particles to the shadows, namely

$$K(R,S) = \psi(R)\Theta(R,S) = \psi(R)\prod_j e^{-C|\mathbf{r}_j - \mathbf{s}_j|^2}. \tag{6}$$

The factors $\psi(R)$ and $\psi_s(S)$ are chosen of the Jastrow form

$$\psi(R)=\prod_{j<l} e^{-1/2\,u(r_{jl})} \text{ and } \psi_s(S)=\prod_{j<l} e^{-u_s(s_{jl})}. \quad (7)$$

The particles pseudopotential $u(r)$ is taken of the McMillan form,

$$u(r)=\left(\frac{b}{r}\right)^5, \quad (8)$$

whereas for the shadows, $u_s(s)$ is taken of the form

$$u_s(s_{jl})=u_s^{\uparrow\uparrow}(s_{jl})\frac{1+\sigma_z(i)\sigma_z(j)}{2}+u_s^{\uparrow\downarrow}(s_{jl})\frac{1-\sigma_z(i)\sigma_z(j)}{2}, \quad (9)$$

where σ_z is the z component of the Pauli matrices. This form of $u_s(s)$ allows for different correlations between spin-parallel and spin-antiparallel pairs. The shadow-shadow pseudopotentials $\{u_s^\sigma|\sigma=\uparrow\uparrow,\uparrow\downarrow\}$ are equal to the two-body interaction potential of the system rescaled in its amplitude and its range by variational parameters:[2]

$$u_s^\sigma(s)=\delta^\sigma V(\alpha^\sigma s). \quad (10)$$

In the case of ^{4}He it has been shown[23] that this choice for the shadow-shadow pseudopotential is significantly better than the McMillan form used in the original computations.

This wave function will hereafter be denoted as shadow-Slater backflow (ShSB) wave function. It is translational invariant and fully antisymmetric under particle exchange. The motivation of the ShSB wave function is based on the assumption that the state-dependent correlations are reasonably well described by backflow correlations. Consequently, the n-body correlations with $n>2$ are basically state independent and therefore can be efficiently treated by means of a shadow-type factor. In fact, the crystallization mechanism is expected to be driven by such many-body correlations, as in ^{4}He. Nevertheless we are aware of the fact that the nodal structure of ShSB trial function is not optimal. Diffusion Monte Carlo calculations, performed fixing the nodal surface of the wave function to that of the Slater backflow function, lead to an equation of state which misses the experimental data by $\sim$10%.[18] Finally, we mention that the Pauli principle induces an effective short range repulsion among particles with parallel spin which should affect their correlation factors. In our wave function this feature was taken into account by the introduction of u_s^σ that are meant to correlate in a different way spin-parallel and spin-antiparallel pairs.

The only variational parameters in the ShSB trial function that have been optimized in this work are C, δ^σ, α^σ, and b. Since the optimization of the backflow parameters at the equilibrium density $\rho\sigma^3=0.273$ ($\sigma=2.556$ Å) have led only to a marginal improvement on the energy upperbound, we have kept the values of Ref. 12 for all the densities considered ($\lambda_B=-1$, $r_B=2.173$ Å, and $w_B=1.278$ Å). We have not attempted, in this exploratory study, to go beyond the McMillan form for the particle-particle pseudopotential and to fully optimize $u(r)$, as done in Ref. 23, following the Euler Monte Carlo method of Refs. 24, 17, and 18.

III. VARIATIONAL MONTE CARLO METHOD

We have computed the energy per particle of ^{3}He at several densities both in the liquid and solid phases,

$$\frac{E}{N}=\left\langle\frac{H\Psi_F}{\Psi_F}\right\rangle, \quad (11)$$

where the angular brackets denote averages taken with respect configurations sampled from the function

$$p(R,S,S')=\phi^2(R)K(R,S)K(R,S')\psi_s(S)\psi_s(S'). \quad (12)$$

In the Hamiltonian of the system

$$H=-\frac{\hbar^2}{2m}\sum\nabla_i^2+\sum_{i<j}V(r_{ij}), \quad (13)$$

the two-body interatomic potential considered is the Hartree-Fock dispersion HFDHE2 potential by Aziz *et al.*[25]

The simulations are performed considering periodic boundary conditions. These conditions determine the wave vectors $\mathbf{k}_i=2\pi\mathbf{n}/L$, where L is the side of our cubic simulation cell and $\mathbf{n}\in Z^3$. To ensure the correct ground state symmetries for the wave function we consider in the simulations a number of particles that fill a complete shell in momentum space. It is well known[22] that single particle moves in the Metropolis random walk is usually the most efficient way for particles to diffuse in the configuration space when the Fermi statistics is enforced without momentum dependent correlations. On the other hand, when dealing with a determinantal wave function that includes backflow, a collective move with an optimized transition probability density gives the lowest variance for a given amount of computer time.[22] For this reason, in our calculations we attempt single moves for the shadows and collective moves for the particles. Most of our simulations were done for 54 atoms. Finite size effects on the binding energy have been estimated at the equilibrium density, using 14, 38, 54, and 66 atoms. They have been found to be of about 0.15 K.

In some of the runs, an additional kind of trial move has been implemented, namely the exchange of particles with different spin assignment. These moves turned out to be very important in the solid phase. The exchange move has been done every 100 ordinary Monte Carlo steps. We have tried to swap pairs of particles randomly chosen. For efficiency reasons, the considered number of such attempts was of the order of the number of particles. The acceptance ratio of this exchange moves has been found to be about 12%.

Other quantities of interest, such as the pair correlation function and the crystalline order parameters have also been computed. The pair correlation function has been decomposed into the spin parallel and spin antiparallel components

$$g_{\uparrow\uparrow,\uparrow\downarrow}(r)=\frac{1}{N\rho}\left\langle\sum_{i,j}^{i\neq j}\frac{1\pm\sigma_z(i)\sigma_z(j)}{2}\delta(r_{ij}-r)\right\rangle, \quad (14)$$

where the plus and minus sign refers to $g_{\uparrow\uparrow}(r)$ and $g_{\uparrow\downarrow}(r)$, respectively. These quantities provide information about the local spin ordering of the system, for both the liquid and solid phases.

In the course of the numerical experiment for the crystallization of the system we have monitored the order parameter

TABLE I. Total and kinetic energy per ^{3}He atom at several densities in the liquid phase (see text).

$\rho(\sigma^{-3})$	$\langle E\rangle/N$ (K)	$\langle T\rangle$ (K)
0.236	-1.838 ± 0.049	9.827 ± 0.063
0.273	-1.821 ± 0.029	11.881 ± 0.040
0.300	-1.563 ± 0.037	14.277 ± 0.050
0.325	-1.182 ± 0.035	15.751 ± 0.047
0.325*	-1.249 ± 0.064	16.224 ± 0.093

$$O_{\{\mathbf{G}\}}=\frac{1}{m_{\{\mathbf{G}\}}N}\left\langle \sum_m \sum_{i=1}^{N} \left| \exp(i\mathbf{G}_m\cdot\mathbf{r}_i)\right|\right\rangle, \qquad (15)$$

where $\{\mathbf{G}\}$ is a star of $m_{\{\mathbf{G}\}}$ vectors in the reciprocal lattice. This was done to ensure that the final averages are taken with respect to configurations that describes really a solid phase. Note that the order parameter as it is defined here is not zero in the disordered phase, but it is $O(1/\sqrt{N})$.

IV. RESULTS

A. Liquid phase

Let us first discuss the results obtained with the ShSB wave function for the liquid phase. In Table I we report the results for the total and kinetic energy at several densities of the liquid phase. These results were obtained with numerical simulations for 54 atoms, keeping the spin-parallel and the spin antiparallel components of $u_s(s)$ equal. At the highest density considered $\rho\sigma^3=0.325$ we have also performed a full minimization, releasing the constraint $\delta^{\uparrow\uparrow}=\delta^{\uparrow\downarrow}$ and $\alpha^{\uparrow\uparrow}=\alpha^{\uparrow\downarrow}$. The improvement in the total energy is only nominal, although the kinetic energy increases considerably (see last line of Table I denoted by 0.325*). For this last case the optimal variational parameters turn out to be $b=1.11\sigma$, $C=3.5\sigma^{-2}$, $\delta^{\uparrow\uparrow}=0.095$ K^{-1}, $\delta^{\uparrow\downarrow}=0.090$ K^{-1}, $\alpha^{\uparrow\uparrow}=0.86$, $\alpha^{\uparrow\downarrow}=0.91$. The optimal values of the variational parameters determined with the constraint $\delta=\delta^{\uparrow\uparrow}=\delta^{\uparrow\downarrow}$ and $\alpha=\alpha^{\uparrow\uparrow}=\alpha^{\uparrow\downarrow}$ are listed in Table II.

The total energy and the kinetic energy per particle at equilibrium density provided by various model trial functions are compared in Table III. For completeness we also report the results obtained with fixed-node diffusion Monte Carlo (DMC) of Refs. 17 and 18. Similarly to what happens for liquid ^{4}He, shadow-type correlations lead to energy upperbound which largely improves upon the results of Jastrow model, and it is just 0.1 K above the energy given by the (J+T)SB model.

TABLE II. Optimal values of the variational parameters of the wave function used in this work with $\delta=\delta^{\uparrow\uparrow}=\delta^{\uparrow\downarrow}$ and $\alpha=\alpha^{\uparrow\uparrow}=\alpha^{\uparrow\downarrow}$.

$\rho(\sigma^{-3})$	$b(\sigma)$	$C(\sigma^{-2})$	δ (K^{-1})	α
		Liquid		
0.236	1.08	3.5	0.095	0.88
0.273	1.08	3.5	0.095	0.88
0.300	1.10	3.5	0.110	0.86
0.325	1.08	3.4	0.090	0.82
		Solid		
0.427	1.08	3.2	0.095	0.81
0.440	1.11	3.2	0.095	0.81

TABLE III. Total and kinetic energy at equilibrium density $\rho\sigma^3=0.273$ for different functional forms of the trial wave function. Calculations from Ref. 21 were done at $\rho\sigma^3=0.277$.

$\langle E\rangle/N$ (K)	$\langle T\rangle$ (K)	Wave function
-1.821 ± 0.029	11.881 ± 0.040	ShSB
-1.08 ± 0.03		JS (Ref. 12)
-1.55 ± 0.04		JSB (Ref. 12)
-1.91 ± 0.03		(J+T)SB (Ref. 12)
-2.163 ± 0.006	12.271 ± 0.008	OJOTB (Ref. 18)
-2.37 ± 0.01		DMC (Ref. 18)

The importance of backflow correlations can be seen comparing JS and Jastrow-Slater-backflow (JSB) models. The values of the backflow parameters in the JSB, (J+T)SB, and ShSB wave functions are the same. Therefore the corresponding energies presented in Table III are directly comparable. The result labeled with OJOTB have been obtained by optimizing both Jastrow and Triplet correlations and using a Slater-backflow wave function for the antisymmetric part.[18] They are not directly comparable with the other results, and have been included for the sake of comparison. The difference between our ShSB and the fixed node DMC result is of the same order of magnitude as the one found in the case of ^{4}He described by the SWF and the Green's function Monte Carlo result.

At the freezing density $\rho\sigma^3=0.325$, the (J+T)SB wave function gives an energy of -1.334 ± 0.052 K, and this is about 0.1 K below the value of ShSB. Thus we do not see here the improvement that shadow wave function gives with respect to J+T in the case of ^{4}He near the freezing point. A possible reason for this feature is the lower value of the freezing density of ^{3}He. Correlations of the shadow-type beyond the triplet level might be less important here. The other possibility is that in the case of a Fermi system these many-body correlations have a significant antisymmetric character, and this feature is not captured by the present shadow wave function.

The spin-parallel and spin-antiparallel components of the pair function at $\rho\sigma^3=0.325$ are displayed in Fig. 1 for the two cases: σ_z-independent and σ_z-dependent shadow-shadow pseudopotential. The σ_z-dependent u_s reduces the short range antiferromagnetic order, in agreement with the DMC results of Ref. 18.

B. Solid phase

Solid ^{3}He is interesting also for its magnetic properties.[26] From experiment we know that below a temperature of the order of the mK a nuclear-spin ordering of the up-up-down-down, etc. form becomes stable, i.e., there is a stacking of two planes of the bcc crystal with up spins, followed by two planes with down spins. Such order is due to a competition between different processes of atomic exchange between two, three, or more atoms. These processes can be hardly observed in standard simulations, and therefore special techniques were developed to overcome this limit.[27] We describe

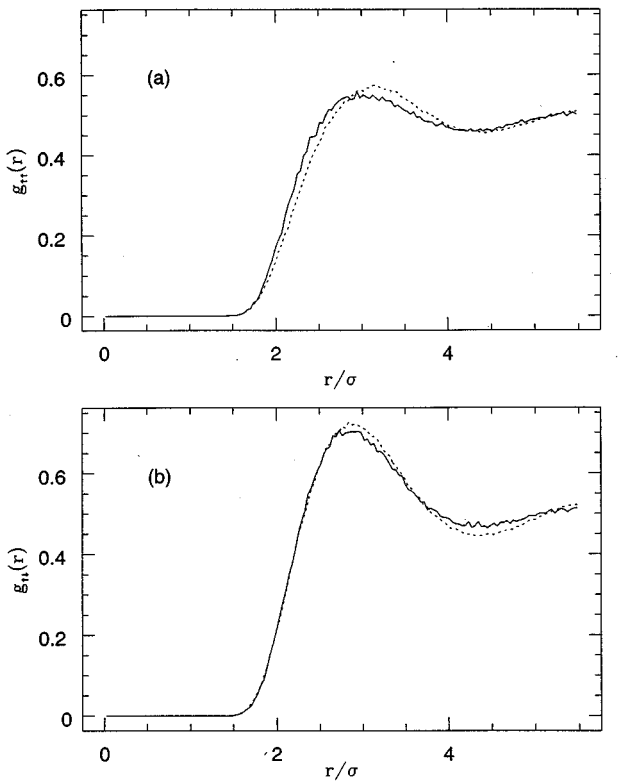

FIG. 1. (a) Spin-parallel $g_{\uparrow\uparrow}(r)$ and (b) spin-antiparallel $g_{\uparrow\downarrow}(r)$ pair functions for liquid ^{3}He at freezing density $\rho\sigma^3=0.325$ for two different parametrizations. Solid lines: $\delta^{\uparrow\uparrow}\neq\delta^{\uparrow\downarrow}$ and $\alpha^{\uparrow\uparrow}\neq\alpha^{\uparrow\downarrow}$; dotted lines: $\delta^{\uparrow\uparrow}=\delta^{\uparrow\downarrow}$ and $\alpha^{\uparrow\uparrow}=\alpha^{\uparrow\downarrow}$. The values of the parameters are given in the text.

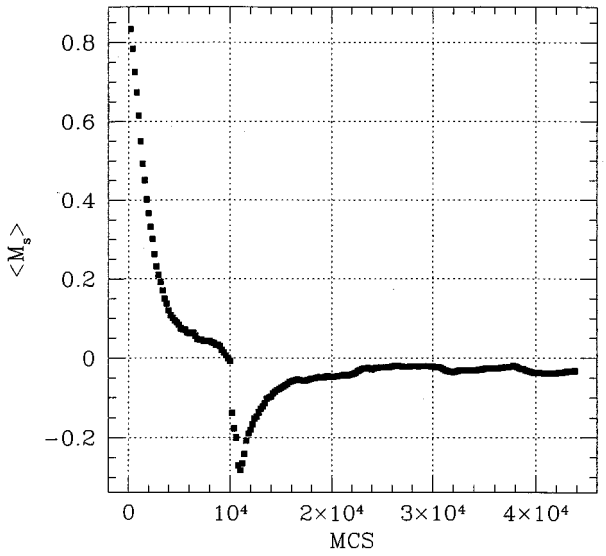

FIG. 2. Averaged staggered magnetization M_s as a function of the number of MCS. The density of the sample is $\rho\sigma^3=0.440$. The jump after 10^4 steps is due to the reset of the estimators after the equilibration phase.

the ^{3}He in the solid phase by the same wave function (1) used for the liquid. As already mentioned, this is a translational invariant wave function that provides spontaneous symmetry breaking at high density. We have performed calculations at two different densities in the solid phase, starting from an initial configuration of the body centered cubic (bcc) type with various magnetic orders. We found that the bcc crystalline order was always stable. We have also performed a simulation starting from a disordered configuration, in order to see if spontaneous crystallization takes place as in ^{4}He.

When the initial configuration has a normal antiferromagnetic order (NAF), we found that such order remained stable during the simulation, because during our finite MC run (about 100 000 steps) all particles stay around their initial positions. The NAF spin ordering gives the lowest energy for the solid (see Table IV). However, this magnetic order did not remain stable when exchange moves were turned on. As discussed in the previous section about 12% of such moves are accepted, and the AF order rapidly decreases from about unity to a value very close to zero, as can be seen in Fig. 2, where the staggered magnetization M_s is plotted as function of the Monte Carlo steps (MCS) performed. The system still shows a prevailing antiferromagnetic local order as it can be seen from the spherically averaged $g(r)$ reported in Fig. 3. The spin-parallel and spin-antiparallel pair function at $\rho\sigma^3=0.440$ resemble those typical of the liquid phase, apart from being more peaked at $r=\sqrt{3}a/2$ for $g_{\uparrow\downarrow}(r)$ and at $r=a$ for $g_{\uparrow\uparrow}(r)$, where a is the unit cell side. The energy for this magnetically disordered state increases by about 1 K over that of the NAF state. Still higher energy is obtained in the case of the fully polarized state, where all spins have the same direction: at density $\rho\sigma^3=0.440$, $\langle E\rangle/N$ is about 4 K.

We can draw the following two conclusions from the results discussed above. In the first place the energy for the NAF state does not correspond to a variational estimate of it, because the very low rate of processes in which particles spontaneously exchange their positions does not allow the system to relax towards a true equilibrium state within the finite length of our MC runs. Similarly, if one used a Nosanow wave function with a frozen spin structure, analogous problems would arise. We are not aware of other computations for solid ^{3}He using the Aziz interatomic potential,

TABLE IV. Total energy and kinetic energy per particle at two densities in the solid phase for different functional forms of the trial wave functions. The value of the order parameter proper for the liquid phase is $\simeq 0.136$.

$\rho\sigma^3$	Wave function	$\langle E\rangle/N$ (K)	$\langle T\rangle$ (K)	$O_{\mathbf{G}}$ (particles)	$O_{\mathbf{G}}$ (shadows)
0.427	ShSB-NAF	0.955±0.033	25.826±0.065	0.291	0.391
	ShSB+exchange	2.057±0.039	25.912±0.069	0.274	0.392
0.440	ShSB-NAF	1.382±0.023	26.511±0.047	0.496	0.725
	ShSB+exchange	2.405±0.042	26.952±0.076	0.426	0.679

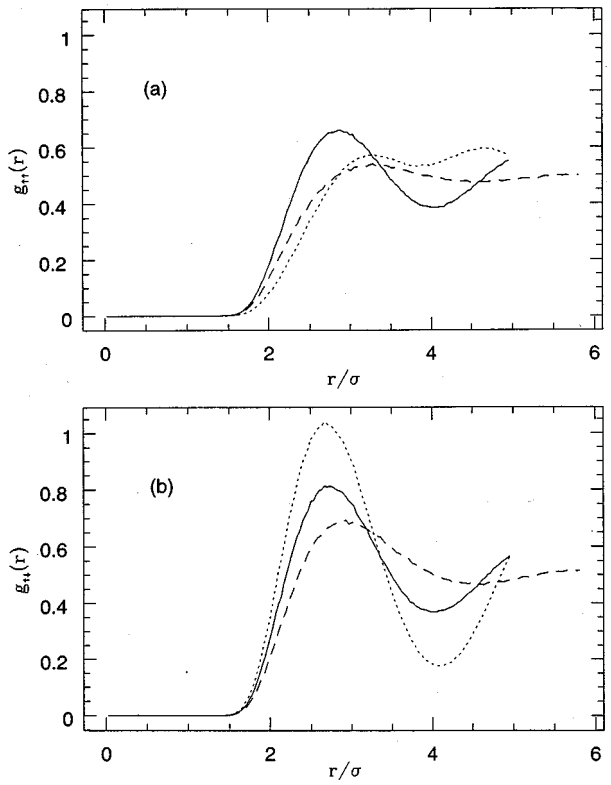

FIG. 3. (a) Spin-parallel $g_{\uparrow\uparrow}(r)$ and (b) spin-antiparallel $g_{\uparrow\downarrow}(r)$ pair functions for liquid ^{3}He at $\rho\sigma^3=0.273$ (dashed lines) and solid ^{3}He at $\rho\sigma^3=0.440$ in the paramagnetic (solid lines) and NAF bcc phase (dotted lines).

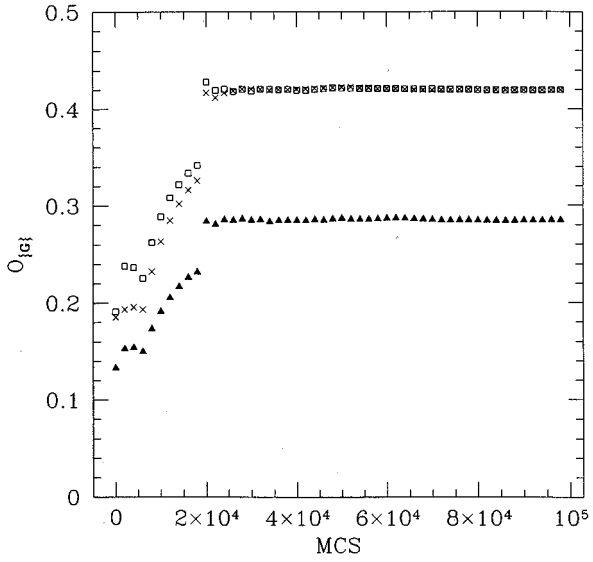

FIG. 4. Evolution of the order parameter for the bcc structure during the numerical simulation of crystallization. Triangles: particles; squares: left shadows; crosses: right shadows. The value of the order parameter in a liquid is ~ 0.136. The discontinuity at 2×10^4 MCS is due to the reset of the estimators after the equilibration phase.

and therefore we cannot compare directly our results. However, at density $\rho\sigma^3=0.427$, a computation performed with a Lennard-Jones potential and a determinant of Gaussians multiplied by a Jastrow term[22] gave an energy of 1.57 K, about 0.5 K lower than our variational result, and about 0.5 K higher than our NAF estimate.

The second conclusion we can draw is that the present wave function overestimates the effect of having different spin configurations on the value of the binding energy. Being the ordering temperature of 1 mK and the Curie temperature of about 2 mK, we should expect the difference in energy amongst different spin configurations not to exceed few mK per particle. This is some orders of magnitude smaller than the difference we find in our computations. Presumably, this is due to the representation of the nodal surface for a solid provided by our shadow wave function. The present nodal structure, strongly dominated by that of the underlying Fermi gas, induces a large Fermi hole between particles with parallel spins. Such an hole does not have a significant effect in the perfect NAF order, because particles with parallel spins are second neighbors and hardly become close to each other. However, the effect of the Fermi hole becomes not negligible as the number of nearest neighbors with parallel spins increases.

In the crystallization simulation, the initial configuration was obtained from a previous simulation of a liquid at equilibrium density $\rho=0.273\sigma^{-3}$, with 54 particles and after 50 000 MCS. It has then been rescaled to obtain the density $\rho=0.44\sigma^{-3}$, well above the melting density. In Fig. 4 we report the value of the order parameter both for particles and shadows during the crystallization run. It can be seen that the value goes from a value of order $1/\sqrt{N}$, typical of a fluid, to a value of order of unity, as expected in a perfect bcc lattice. The fact that this value never reaches 1 is due to quantum fluctuations of particles around the lattice sites, in full analogy with the simulations performed for ^{4}He. The obtained energy per particle 3.048 ± 0.023 K is about 0.6 K higher than that found when starting from a bcc configuration. This difference is analogous to that observed in the case of ^{4}He.[4] In that case such difference was explained by the fact that in the crystallization run the particles have frozen with the crystal axes tilted with respect to the simulation box axes. This feature, together with the periodic boundary conditions, induces defects and deformations in the crystalline order. The analysis of the configurations shows that also in the present case the crystalline order is not grown parallel to the simulation box axes.

V. CONCLUSIONS

We have presented results for liquid and solid ^{3}He based on the shadow wave function. In the present wave function only many-body correlations of symmetric character are introduced by the shadow variables. In the liquid phase we find a significant improvement in the energy compared to the case of pure Jastrow correlations. A comparison with the energy upperbounds yielded by (J+T)SB wave function seems to indicate that symmetric correlations beyond the triplet level are less important in ^{3}He than in ^{4}He or else that such many-body correlations should have an important antisymmetric character.

The most important feature of our shadow wave function is the possibility of describing solid ^{3}He without introducing *a priori* equilibrium positions. Indeed, we have found that ShSB wave function is able to provide a stable crystalline

order, even starting from a liquidlike configuration of the atoms. Therefore, the many-body correlations of the shadow type, at sufficiently high density, introduce a spontaneously broken translational symmetry. Moreover, the ShSB wave functions can be easily generalized to include density dependent parameters,[9] to describe inhomogeneous systems. Computer simulations for liquid-solid coexistence, which requires a large number of ^{3}He atoms, are at the reach of the present computational capabilities.

Finally, we have we also found a strong dependence of the energy on the configuration of the spins in the solid phase, which indicates that the magnetic properties of solid ^{3}He are very sensitive to the nodal structure of our wave function. The Fermi hole brought in by the nodal structure of our wave function, which has a small effect in the perfect NAF state, becomes more and more important when some nearest neighbors with parallel spins are present. We expect that this problem will be better clarified with a shadow wave function in which the antisymmetric part is written in terms of the shadow variables. It has been shown[28] that in this last case the nodal structure changes from that of a Fermi gas to that of a determinant of Gaussians, depending on the density and on the coupling parameters. This new form of the trial wave function should provide enough flexibility to give a more satisfactory description of the solid phase. Work in this direction is in progress.

ACKNOWLEDGMENT

The authors would like to acknowledge many useful discussions with M. H. Kalos.

[1] S.A. Vitiello, K. Runge, and M.H. Kalos, Phys. Rev. Lett. **60**, 1970 (1988).
[2] L. Reatto and G.L. Masserini, Phys. Rev. B **38**, 4516 (1988).
[3] S.A. Vitiello, K. Runge, G.V. Chester, and M.H. Kalos, Phys. Rev. B **42**, 228 (1990).
[4] F. Pederiva, A. Ferrante, S. Fantoni, and L. Reatto, Phys. Rev. B **52**, 7564 (1995).
[5] W. Wu, S.A. Vitiello, L. Reatto, and M.H. Kalos, Phys. Rev. Lett. **67**, 1446 (1991).
[6] L. Reatto, S.A. Vitiello, and G.L. Masserini, J. Low Temp. Phys. **93**, 879 (1993).
[7] L. Reatto, G.L. Masserini, and S.A. Vitiello, Physica B **197**, 189 (1994).
[8] G.L. Masserini, L. Reatto, and S.A. Vitiello, Phys. Rev. Lett. **69**, 2098 (1992).
[9] F. Pederiva, A. Ferrante, S. Fantoni, and L. Reatto, Phys. Rev. Lett. **72**, 2589 (1994); Physica B **194**, 967 (1994).
[10] F. Pederiva, S. Fantoni, and L. Reatto, J. Low Temp. Phys. **101**, 541 (1995).
[11] E. Feenberg, *Theory of Quantum Fluids* (Academic Press, New York, 1969).
[12] K.E. Schmidt, M.A. Lee, M.H. Kalos, and G.V. Chester, Phys. Rev. Lett. **47**, 807 (1981).
[13] E. Manousakis, S. Fantoni, V.R. Pandharipande, and Q.N. Usmani, Phys. Rev. B **28**, 3770 (1983).
[14] M. Viviani, E. Buendia, S. Fantoni, and S. Rosati, Phys. Rev. B **38**, 4523 (1988).
[15] L. Reatto, in *Recent Progress in Many-Body Theories*, edited by T.L. Ainsworth *et al.* (Plenum, New York, 1992).
[16] A. Ferrante, M. Bernasconi, X.Q.G. Wang, S. Fantoni, and E. Tosatti, in *Many-Body Theories*, edited by T.L. Ainsworth *et al.* (Plenum, New York, 1992), p. 233.
[17] S. Moroni, S. Fantoni, and G. Senatore, Europhys. Lett. **30**, 93 (1995).
[18] S. Moroni, S. Fantoni, and G. Senatore, Phys. Rev. B **52**, 13 547 (1995).
[19] L.H. Nosanow and G.L. Shaw, Phys. Rev. **128**, 546 (1962).
[20] L.H. Nosanow, Phys. Rev. **146**, 120 (1966).
[21] J.P. Hansen and D. Levesque, Phys. Rev. **165**, 293 (1968).
[22] D. Ceperley, G.V. Chester, and M.H. Kalos, Phys. Rev. B **16**, 3081 (1977).
[23] T. MacFarland, S.A. Vitiello, L. Reatto, G.V. Chester, and M.H. Kalos, Phys. Rev. B **50**, 13 577 (1994).
[24] S.A. Vitiello and K.E. Schmidt, Phys. Rev. B **46**, 5442 (1992).
[25] R.A. Aziz, V.P.S. Nain, J.S. Carley, W.L. Taylor, and G.T. McConville, J. Chem. Phys. **70**, 4330 (1970).
[26] D.D. Osheroff, J. Low Temp. Phys. **87**, 297 (1992), and references therein.
[27] D.M. Ceperley and G. Jacucci, Phys. Rev. Lett. **58**, 1648 (1987).
[28] M.H. Kalos and L. Reatto, in *Progress in Computational Physics of Matter*, edited by L. Reatto and F. Manghi (World Scientific, Singapore, 1995), p. 99.